Generating Stable Spin Squeezing by Squeezed-Reservoir Engineering

Si-Yuan Bai and Jun-Hong An*
Lanzhou Center for Theoretical Physics, Key Laboratory of Theoretical Physics of Gansu Province, Lanzhou University, Lanzhou 730000, China

(Received 23 March 2021; revised 13 July 2021; accepted 26 July 2021; published 17 August 2021; corrected 19 August 2021)

As a genuine many-body entanglement, spin squeezing (SS) can be used to realize the highly precise measurement beyond the limit constrained by classical physics. Its generation has attracted much attention recently. It was reported that N two-level systems (TLSs) located near a one-dimensional waveguide can generate SS by using the mediation effect of the waveguide. However, a coherent driving on each TLS is used to stabilize the SS, which raises a high requirement for experiments. We here propose a scheme to generate stable SS resorting to neither the spin-spin coupling nor the coherent driving on the TLSs. Incorporating the mediation role of the common waveguide and the technique of squeezed-reservoir engineering, our scheme exhibits the advantages over previous ones in the scaling relation of the SS parameter with the number of the TLSs. The long-range correlation feature of the generated SS along the waveguide in our scheme may endow it with certain superiority in quantum sensing, e.g., improving the sensing efficiency of spatially unidentified weak magnetic fields.

DOI: 10.1103/PhysRevLett.127.083602

Introduction.—A quantum-science revolution is in the making. It is expected to bring a lot of profound impacts to technological innovations. A distinguished example is quantum metrology or sensing [1,2]. It pursues the development of measurement protocols with higher precision of physical quantities than the limit constrained by classical physics, i.e., the shot-noise limit, by using quantum resources. As a kind of many-body entanglement [3–6], spin squeezing (SS) is one such resource. It has exhibited a wonderful power in beating the shot-noise limit [7–13], with promising applications in quantum gyroscope [14,15], atomic clocks [16–20], magnetometers [21,22], and gravimetry [23]. Its efficient generation is a prerequisite for further applications. The widely used method exploits the coherent spin-spin coupling in the one- and two-axis twisting models [4,7–10,24]. However, it is dynamically transient and experiences a degradation under the realistic decoherence [25–27]. Other methods via atom-photon couplings [28–31] and quantum nondemolition measurements [32–34] have also been proposed.

Waveguide quantum electrodynamics (QED) refers to a scenario where arrays of quantum emitters are coupled to a waveguide [35–42]. It allows for long-range interactions among the quantum emitters mediated by photons in the waveguide that is particularly interesting for quantum network applications [43]. Several schemes on dissipative preparation of the SS [44–51] have been proposed based on the idea of reservoir engineering [52–56] to the waveguide modes. The SS generated in such a method exists in steady states and does not depend on initial states, which endows it with the features of a long lifetime and robustness. However, a coherent driving laser on each quantum emitter is needed to stabilize the SS in these schemes. It dramatically increases the experimental difficulties when a huge number of quantum emitters are involved.

In this Letter, we propose a scheme to deterministically generate a stable SS of N distant quantum emitters formed by two-level systems (TLSs) in a waveguide QED system without resorting to a coherent driving on each TLS. The main idea is based on the combined action of the technique of squeezed-reservoir engineering, which is widely used in quantum state preparation [57–62], and the mediation role of the waveguide. The waveguide enables us to manipulate the phase difference between the reservoir-induced long-range coherent and incoherent couplings of TLSs such that an effective collective spin mode of TLSs is induced by precisely controlling the positions of TLSs. Then, acting as a mold, the squeezed-reservoir imprints its squeezing feature to the steady state of the collective spin. It is found that the Wineland SS parameter ξ_R^2, as a characterization of the improvement of sensitivity in Ramsey spectroscopy [3], for our generated SS scales with the TLS number N as $1.64N^{-0.54}$, which beats the ones in the one- and two-axis twisting [25–27] and Heisenberg [63] models with the realistic dissipation considered. It implies the superiority of the SS of our scheme in quantum sensing. The spatial separation of the TLSs along the waveguide in our scheme also is helpful in improving the sensing efficiency of a weak field via effectively increasing the contact area.

System and dynamics.—We consider an array of N TLSs coupled to a common electromagnetic field in a waveguide [see Fig. 1(a)]. The TLSs can be superconductor qubits [64], nitrogen vacancy centers [50], or natural atoms [65]. The waveguide may be a coupled cavity array [66], a

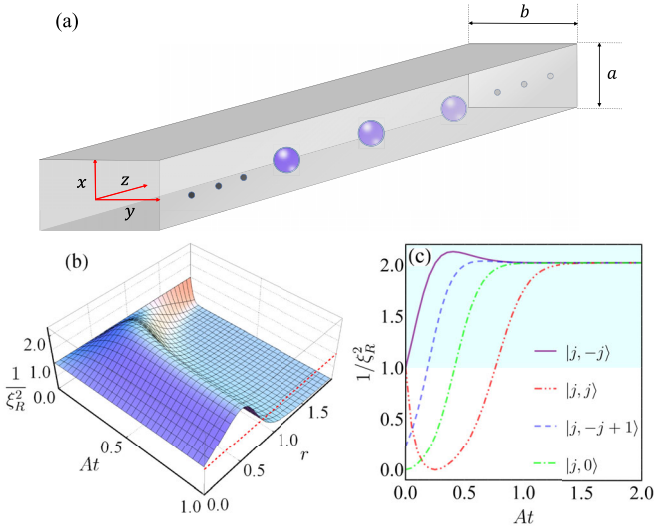

FIG. 1. (a) Schematics of N TLSs along z axis in a one-dimensional waveguide, which is driven by a broadband squeezed field. Evolution of the inverse of the SS parameter of the TLSs in different r when the initial state is $|j,-j\rangle$ with $j=N/2$ (b) and in different initial states when $r=0.5$ (c). The red dashed line in (b) denotes $\xi_R^2=1$. Other parameters are $N=10$, $\omega_0=\Delta=1.0A$, and $\alpha=0.5$.

metal-dielectric surface plasmon [67,68], or a photonic crystal [69]. Its Hamiltonian is $\hat{H}=\hat{H}_S+\hat{H}_R+\hat{H}_I$ with ($\hbar=1$)

$$\hat{H}_S=\sum_{i=1}^{N}\omega_0\hat{\sigma}_i^\dagger\hat{\sigma}_i,\qquad \hat{H}_R=\sum_k\omega_k\hat{a}_k^\dagger\hat{a}_k, \tag{1}$$

$$\hat{H}_I=\sum_{k,i}(g_{ki}\hat{a}_k+g_{ki}^*\hat{a}_k^\dagger)(\hat{\sigma}_i^\dagger+\hat{\sigma}_i), \tag{2}$$

where $\hat{\sigma}_i$ is the transition operator from the excited state $|e\rangle$ to the ground state $|g\rangle$ of the ith TLS at $\mathbf{r}_i$, with transition frequency ω_0, and $\hat{a}_k$ is the annihilation operator of the kth field mode with frequency ω_k. The coupling strength is $g_{ki}=\sqrt{\omega_k/(2\epsilon_0)}\mathbf{d}_i\cdot\mathbf{u}_k(\mathbf{r}_i)$, where ϵ_0 is the vacuum permittivity, $\mathbf{d}_i$ is the dipole moment of the ith TLS, and $\mathbf{u}_k(\mathbf{r}_i)$ is the spatial function of the kth mode.

We use the technique of squeezed-reservoir engineering [58–62] to generate the SS of TLSs. It is realized by feeding the waveguide a broadband squeezed field, which can be implemented via an optical parametric down conversion [70,71] or Josephson parametric amplification [72,73]. The waveguide under the driving of the squeezed field acts as a squeezed vacuum reservoir. The initial state is $\rho_T(0)=\rho(0)\otimes\prod_k\hat{S}_k|0_k\rangle\langle 0_k|\hat{S}_k^\dagger$, where $\hat{S}_k=\exp[r_k(e^{-i\alpha_k}\hat{a}_k^2-e^{i\alpha_k}\hat{a}_k^{\dagger 2})/2]$ with r_k and α_k being the squeezing strength and angle, and $|0_k\rangle$ is the kth-mode vacuum state [57]. Both r_k and α_k relate to the amplitude of the pump field, the second-order nonlinearity, and the length of nonlinear material in parametric amplification. The master equation of the TLSs under the Born-Markovian and secular approximations is [74–76]

$$\begin{aligned}\dot{\tilde{\rho}}(t)=&-i\Big[\Delta_{\mathcal{N}}\sum_i\hat{\sigma}_i^\dagger\hat{\sigma}_i+\hat{H}_{\mathrm{DD}},\tilde{\rho}(t)\Big]\\&+\sum_{i,j}\{\gamma_{ij}^-/2[\mathcal{N}\check{\mathcal{D}}_{\hat{\sigma}_i^\dagger,\hat{\sigma}_j}+(\mathcal{N}+1)\check{\mathcal{D}}_{\hat{\sigma}_i,\hat{\sigma}_j^\dagger}]\\&-\gamma_{ij}^+/2[\mathcal{M}\check{\mathcal{D}}_{\hat{\sigma}_i^\dagger,\hat{\sigma}_j^\dagger}+\mathcal{M}^*\check{\mathcal{D}}_{\hat{\sigma}_i,\hat{\sigma}_j}]\}\tilde{\rho}(t),\end{aligned} \tag{3}$$

where $\tilde{\rho}(t)=e^{i\hat{H}_S t}\rho(t)e^{-i\hat{H}_S t}$ is the density matrix of TLSs in the interaction picture, $\mathcal{N}\equiv\sinh^2 r$ with $r\equiv r(\omega_0)$, $\mathcal{M}\equiv\sqrt{\mathcal{N}^2+\mathcal{N}}e^{i\alpha}$ with $\alpha\equiv\alpha(\omega_0)$, and $\check{\mathcal{D}}_{\hat{A},\hat{B}}\tilde{\rho}\equiv 2\hat{A}\,\tilde{\rho}\,\hat{B}-\tilde{\rho}\,\hat{B}\,\hat{A}-\hat{B}\,\hat{A}\,\tilde{\rho}$. The first term of Eq. (3) is the reservoir-induced coherent dynamics, where $H_{\mathrm{DD}}=-\sum_{i\neq j}\Delta_{ij}(\hat{\sigma}_i^\dagger\hat{\sigma}_j+\hat{\sigma}_i\hat{\sigma}_j^\dagger)/2$ is the dipole-dipole interaction of the TLSs. The interaction strengths are $\Delta_{ij}=\Delta_{ij}^-+\Delta_{ij}^+$ with $\Delta_{ij}^\pm=\mathcal{P}\int_0^\infty d\omega G_{ij}^-(\omega)/(\omega\pm\omega_0)$, where $\mathcal{P}$ denotes the Cauchy principal value and $G_{ij}^-(\omega)\equiv\sum_k g_{ki}g_{kj}^*\delta(\omega-\omega_k)$ are the correlated spectral densities. The frequency shift equals to $\Delta_{\mathcal{N}}\equiv(2\mathcal{N}+1)\Delta$ with $\Delta=(\Delta_{ii}^+-\Delta_{ii}^-)$, which is independent of the positions of TLSs. The second and third lines of Eq. (3) are the incoherent dissipation and squeezing with rates $\gamma_{ij}^\pm=2\pi G_{ij}^\pm(\omega_0)$, where $G_{ij}^+(\omega)\equiv\sum_k g_{ki}g_{kj}\delta(\omega-\omega_k)$. It is interesting to see that the squeezed vacuum reservoir, as a common medium of the TLSs, can not only induce individual dissipation, squeezing, and frequency shift to each TLSs, but also induce correlated dissipation, squeezing, and coherent dipole-dipole interactions to the TLSs by exchanging the photons in the waveguide. It gives us sufficient room to generate a long-range correlation of TLSs via engineering the reservoir in the waveguide.

The surface plasmonic as a waveguide experiences severe loss due to the metal absorption [67]. The photonic crystal as a waveguide reflects light only in a certain narrow frequency range [69]. We consider that the waveguide is formed by a rectangular hollow metal due to its high Q factor [77] and wide permissable bandwidth. Its allowable electromagnetic modes are the transverse modes TE_{mn} and TM_{mn} above the cutoff frequency $\omega_{mn}=c[(m\pi/a)^2+(n\pi/b)^2]^{1/2}$, where a, b are the transverse lengths of the waveguide, and m, n are nonnegative integers. Their dispersion relations are $\omega_k^{mn}=[(ck)^2+\omega_{mn}^2]^{1/2}$ with k being the longitudinal wave number and c being the speed of light [78]. Assuming that the TLSs are polarized in the z direction ($\mathbf{d}_i=d\mathbf{e}_z$), we have [45]

$$G_{ij}^\pm(\omega)=\sum_{mn}\frac{\Gamma_{mn}}{2\pi}\frac{\cos[k(z_i\pm z_j)]}{[(\omega/\omega_{mn})^2-1]^{1/2}}\Theta(\omega-\omega_{mn}) \tag{4}$$

with $\Theta(x)$ as the Heaviside step function, $\Gamma_{mn}=[(4\omega_{mn}\tilde{u}_{mn,i}\tilde{u}_{mn,j})/(\epsilon_0 cab)]$, and $\tilde{u}_{mn,i}=d\sin[(m\pi/a)x_i]\times\sin[(n\pi/b)y_i]$. Considering the dominated mode with $m=n=1$ and $\omega_0>\omega_{11}$, we can derive [76]

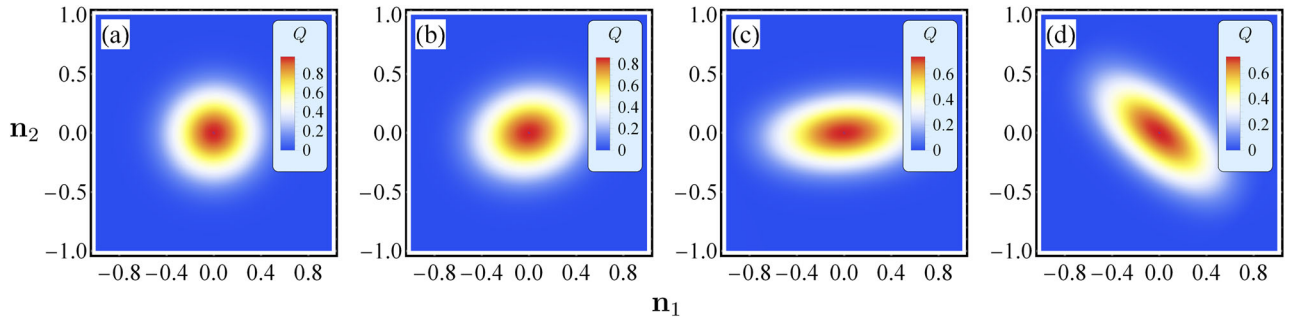

FIG. 2. Evolution of the Husimi's Q function in the $\mathbf{n}_\perp$ plane for the initial state $|j,-j\rangle$ when $t=0$ (a), $0.01A^{-1}$ (b), $0.1A^{-1}$ (c), and $t=4.0A^{-1}$ (d). We use $N=30$ and $r=0.8$, and others are the same as Fig. 1.

$$\Delta_{ij} = -[\Gamma_{11}\zeta\omega_{11}/(2c)]\sin(|z_i - z_j|/\zeta), \tag{5}$$

$$\gamma_{ij}^{\pm} = (\Gamma_{11}\zeta\omega_{11}/c)\cos(|z_i \pm z_j|/\zeta), \tag{6}$$

where $\zeta = c(\omega_0^2 - \omega_{11}^2)^{-1/2}$. Equations (5) and (6) originate from the interference of the N individual interaction channels of the TLSs with the common reservoir [66]. Remarkably, the waveguide as the reservoir medium enables us to modulate the phase difference of Eqs. (5) and (6) via tailoring the position z_i. It allows the switch-on-off for either of the two couplings and offers an opportunity for engineering the multipartite quantum correlation of the TLSs. By positioning the TLSs such that $|z_i \pm z_j| = 2n_\pm\pi\zeta$ ($n_\pm \in \mathbb{Z}$), we have $\Delta_{ij}=0$, $\gamma_{ij}^{\pm} = \Gamma_{11}\zeta\omega_{11}/c \equiv A$, and Eq. (3) reduced to [76]

$$\dot{\tilde{\rho}}(t) = -i\Delta_{\mathcal{N}}[\hat{S}^z, \tilde{\rho}(t)] + \frac{A}{2}[\mathcal{N}\check{\mathcal{D}}_{\hat{S}^+,\hat{S}^-} + (\mathcal{N}+1)\check{\mathcal{D}}_{\hat{S}^-,\hat{S}^+} - \mathcal{M}\check{\mathcal{D}}_{\hat{S}^+,\hat{S}^+} - \mathcal{M}^*\check{\mathcal{D}}_{\hat{S}^-,\hat{S}^-}]\tilde{\rho}(t), \tag{7}$$

where $\hat{S}^z \equiv \sum_i(\hat{\sigma}_i^\dagger\hat{\sigma}_i - 1/2)$ and $\hat{S}^- = (\hat{S}^+)^\dagger = \sum_i \hat{\sigma}_i$. Thus, a collective spin mode of the TLSs is induced to interplay with the common squeezed reservoir by the constructive interference among the interaction channels.

Stable spin squeezing.—An SS is featured with a reduced quantum fluctuation in a certain spin component. Defining a mean direction $\mathbf{n} = \mathrm{Tr}(\hat{\mathbf{S}}\rho)/|\mathrm{Tr}(\hat{\mathbf{S}}\rho)| \equiv (\sin\theta_0\cos\varphi_0, \sin\theta_0\sin\varphi_0, \cos\theta_0)$, a spin state ρ is squeezed if its minimal variance in the $\mathbf{n}_\perp$ plane spanned by $\mathbf{n}_1 = (\cos\theta_0\cos\varphi_0, \cos\theta_0\sin\varphi_0, -\sin\theta_0)$ and $\mathbf{n}_2 = (-\sin\varphi_0, \cos\varphi_0, 0)$ is smaller than that of the spin coherent state, i.e., $N/4$ [4]. It is quantified by the SS parameter [3] $\xi_R^2 = N[\mathrm{Var}(\hat{\mathbf{S}}^\perp)]_{\min}/|\mathrm{Tr}(\hat{\mathbf{S}}\rho)|^2$, where $\hat{\mathbf{S}}^\perp$ is the spin in the $\mathbf{n}_\perp$ plane, $\mathrm{Var}(\hat{O}) = \langle\hat{O}^2\rangle - \langle\hat{O}\rangle^2$, and the superscript min means the minimum in all directions. Exhibiting multipartite entanglement, the state is squeezed if $\xi_R^2 < 1$ [79]. Another way to visually depict the SS is the Husimi's Q function $Q(\theta,\varphi) = (2j+1)/(4\pi)\langle\theta,\varphi|\rho|\theta,\varphi\rangle$ [80], where $|\theta,\varphi\rangle = (1+|\eta|^2)^{-j}e^{-\eta^*\hat{S}^-}|j,j\rangle$ with $|j,m\rangle$ ($m=-j,\ldots,j$) being the eigenstates of $\{\hat{\mathbf{S}}^2, \hat{S}^z\}$ and $\eta = -\tan(\theta/2)e^{-i\varphi}$. The Q function maps ρ to a quasiclassical probability distribution in the phase space defined by θ and φ.

Via numerically solving Eq. (7), we show in Fig. 1(b) the evolution of $1/\xi_R^2$ for the initial state $|j,-j\rangle$ with $j=N/2$ in different squeezing strengths r. It is found that a stable SS can be formed in the regime of a moderate r. Thanks to the constructive role played by the squeezed reservoir in the waveguide, the system spontaneously evolves to a spin squeezed state uniquely dependent on r. This is in sharp contrast to the previous results [47–51], where a coherent driving field is applied on each TLS to stabilize the SS. The evolution of $1/\xi_R^2$ with chosen r in different initial states $|j,m\rangle$ verifies the uniqueness of the steady state [see Fig. 1(c)]. We plot in Fig. 2 the evolution of the projections of the Q function in the $\mathbf{n}_\perp$ plane for the initial state $|j,-j\rangle$. Being isotropically distributed, it shows no SS initially. With increasing time, it shrinks in one direction at the expense of expanding in its orthogonal direction. Such an SS is kept to its steady state [see Fig. 2(d)]. It confirms that the TLSs as a collective spin are squeezed by the squeezed reservoir.

To figure out the relation between the SS and r, we calculate the steady state [76,81]

$$\tilde{\rho}(\infty) = \sum_{m,n=-j}^{j} p_m p_n^* \langle\phi_m|\phi_n\rangle|\psi_m\rangle\langle\psi_n|. \tag{8}$$

Satisfying $\hat{R}_z|\psi_m\rangle = m|\psi_m\rangle$ and $\hat{R}_z^\dagger|\phi_m\rangle = m|\phi_m\rangle$ with $\hat{R}_z = i(4|\mathcal{M}|)^{-1/2}(\hat{S}^+e^{i(\alpha/2)}\sinh r - \hat{S}^-e^{-i(\alpha/2)}\cosh r)$, $|\psi_m\rangle$ and $|\phi_m\rangle$ forms a complete set of biorthogonal basis. The recurrence relation of coefficient p_m is $p_{m+1} = \{[Am - i\Delta_{\mathcal{N}}]/[A(m+1) + i\Delta_{\mathcal{N}}]p_m\}$, which can be fixed by $\mathrm{Tr}[\tilde{\rho}(\infty)] = 1$.

We plot in Fig. 3(a) the comparison of the steady-state squeezing obtained by the analytical solution (8) with the numerical one. It verifies the correctness of Eq. (8) in describing the steady state of Eq. (7). One observation from Fig. 3(a) is that, with increasing N, the range of r supporting the stable SS becomes wider and wider. Thus, the stable SS can be generated in a fairly wider parameter range if more TLSs are involved [see Fig. 3(b)]. Another feature of Fig. 3(a) is that, even for sufficiently

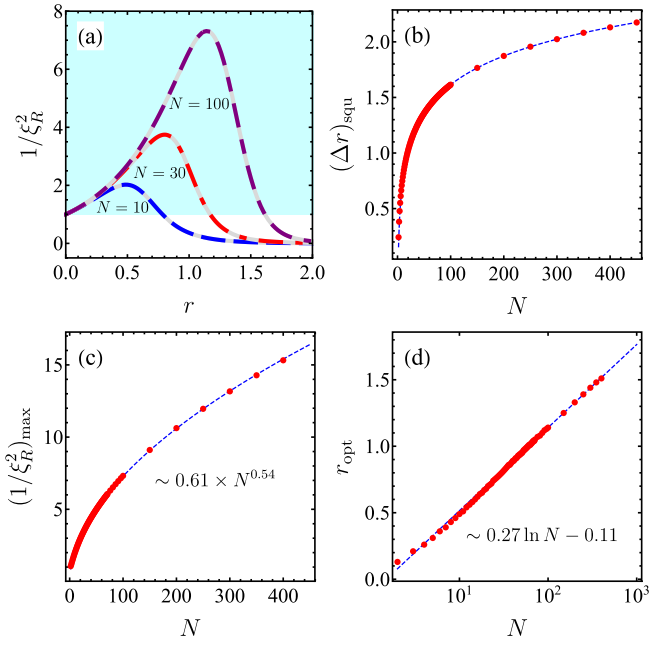

FIG. 3. (a) Comparison of $1/\xi_R^2$ from the analytical solution (8) (purple dot dashed, red dashed, and blue dotted lines) with the one by numerically solving Eq. (7) at $t = 200A^{-1}$ (gray lines) in different N. Range of r supporting stable SS (b), maxima of $1/\xi_R^2$ (c), and optimal r (d) as a function of N. The numerical fitting gives $(\xi_R^2)_{\rm Max} = 1.64N^{-0.54}$ and $r_{\rm opt} = 0.27 \ln N - 0.1$. Parameters are the same as Fig. 1.

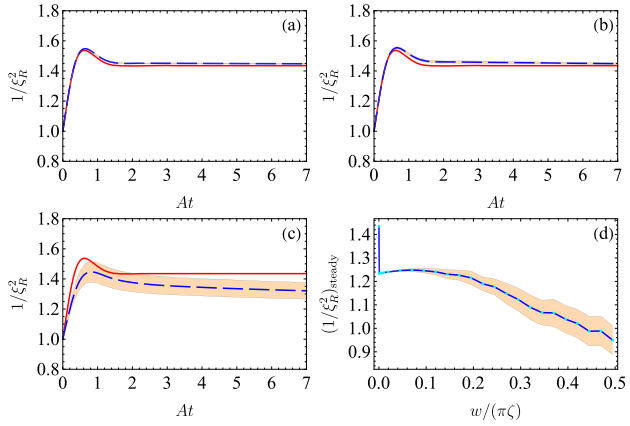

FIG. 4. Evolution of $1/\xi_R^2$ in the ideal (red line) and disordered (blue dashed line) cases with the standard deviations marked in orange when $w = 0.03\pi\zeta$ (a), $0.06\pi\zeta$ (b), and $0.3\pi\zeta$ (c) by averaging over 100 random configurations. (d) Steady-state $1/\xi_R^2$ in different w by averaging over 200 random configurations. $N = 5$ and others are the same as Fig. 1.

large N, the SS still tends to vanish in a gradual manner with increasing r. It endows our scheme with a difference from the previous ones based on the driven-dissipative Dicke model [47,50], where a nonequilibrium phase transition manifested by an abrupt disappearance of the SS is presented. It is understandable based on the fact that our SS is generated via purely incoherent interactions of TLSs mediated by the reservoir, while theirs is via the combined actions of the incoherent interactions and coherent driving.

The SS parameter ξ_R^2 describes the improvement of the sensitivity to measure the atomic frequency in Ramsey spectroscopy [3]. Therefore, it itself is an important quantity to characterize quantum superiority in quantum metrology [82–85]. The analytical solution (8) permits us to investigate the SS in the large-N limit, where the numerical calculation is hard. The relation between the optimal SS and the number N of the TLSs is calculated via Eq. (8) [see red dots in Fig. 3(b)]. Via numerical fitting, we obtain its scaling relation as

$$(\xi_R^2)_{\rm min} = 1.64 \times N^{-0.54}. \tag{9}$$

According to the definition of ξ_R^2 [3], the metrology error using this state in Ramsey spectroscopy outperforms the shot-noise limit achieved using the spin coherent state by a factor of $\sqrt{1.64}N^{-0.27}$. It is better than the previous schemes. Explicitly, the SS generated via the one-axis twisting scales as $\xi_R^2 \propto N^{-2/3}$ and via two-axis twisting as N^{-1} in the ideal situation [4]. However, they tend to $N^{-1/2}$ at optimized time and to be divergent in the long-time limit when the dissipation is considered [25–27]. Our SS is also better than the ones in the ground state of Lipkin-Meshkov-Glick model scaling as $\xi_R^2 \propto N^{-1/3}$ [86] and in the steady state of dissipative Heisenberg model scaling as $\xi_R^2 = 1/2$ [63]. Figure 3(c) shows the squeezing strength to achieve the best SS in different N. The numerical fitting reveals $r_{\rm opt} = 0.27 \ln N - 0.11$ [76], which insensitively depends on N. Thus, we do not bother to sharply increase r to generate the SS for a large number of TLSs. This gives a useful guideline for experiments to optimize the working condition.

Effect of position imperfection.—Consider that the position z_i of ith TLS has a disorder $w\chi_i$, where χ_i is a random number uniformly distributed in $[-1, 1]$ and w is disorder strength. The disorder makes the collective spin mode in Eq. (7) not exist anymore. Solving the original master equation (3), we plot in Figs. 4(a)–4(c) the evolution of $1/\xi_R^2$ in different w. It can be found that the disorder introduces a decay factor roughly in a timescale $\zeta/(Aw)$ to $1/\xi_R^2$ [76]. When w is small, almost no observable influence can be found in a sufficiently wide time window. With increasing w, the decay becomes obvious. By setting the left-hand side of Eq. (3) to zero, we plot in Fig. 4(d) the steady-state $1/\xi_R^2$ in different w. It shows that the stable SS is preserved until the disorder strength is as high as $0.4\pi\zeta$. This reveals the robustness of our scheme to the position imperfection of the TLSs.

Discussion and conclusion.—The current experimental advances in nanophotonics and circuit QED provide support to our scheme [36–40]. The transmission-line

waveguide mediated couplings of two 18.6 mm separated TLSs have been observed [36]. A 15 dB squeezed light corresponding to $r = 1.7$ has been realized [70]. A 20 dB squeezing for microwave with bandwidth up to a few GHz has been realized by the Josephson parametric amplifier [73], which fulfills our requirement. The precise positioning of TLSs with 20 nm accuracy was reported [87,88]. Our scheme is also realizable in SiV centers as TLSs in a diamond waveguide [43,55,89]. Comparing with the SS in an atom ensemble [7–13], our SS shows a long-range correlation. It hopefully is useful in developing quantum sensing in extremal conditions, e.g., improving the sensing efficiency of a spatially unidentified weak magnetic field via effectively increasing the contact area.

In summary, we have proposed a scheme to generate stable SS of N distant TLSs in a waveguide QED system by squeezed-reservoir engineering. A collective effect of the far separated TLSs is efficiently created by the mediation role of the common squeezed reservoir in the waveguide via well-positioned TLSs. It makes the TLSs spontaneously evolve from any initial state to a spin squeezed state in the long-time limit. Our analysis reveals that the generated SS scales with the number of TLSs as $N^{-0.54}$, which outperforms the two-axis twisting and Heisenberg models with the realistic dissipation considered. Without resorting to the coherent driving on each TLS, our scheme reduces the difficulty of experiment realization in previous schemes. The recent advancement of the waveguide QED experiments indicates that our scheme is within the present experimental state of the art.

This work is supported by the National Natural Science Foundation (Grants No. 11875150, No. 11834005, and No. 12047501).

*anjhong@lzu.edu.cn

[1] C. L. Degen, F. Reinhard, and P. Cappellaro, Quantum sensing, Rev. Mod. Phys. **89**, 035002 (2017).
[2] L. Pezzè, A. Smerzi, M. K. Oberthaler, R. Schmied, and P. Treutlein, Quantum metrology with nonclassical states of atomic ensembles, Rev. Mod. Phys. **90**, 035005 (2018).
[3] D. J. Wineland, J. J. Bollinger, W. M. Itano, F. L. Moore, and D. J. Heinzen, Spin squeezing and reduced quantum noise in spectroscopy, Phys. Rev. A **46**, R6797 (1992).
[4] M. Kitagawa and M. Ueda, Squeezed spin states, Phys. Rev. A **47**, 5138 (1993).
[5] B. Lücke, J. Peise, G. Vitagliano, J. Arlt, L. Santos, Géza Tóth, and C. Klempt, Detecting Multiparticle Entanglement of Dicke States, Phys. Rev. Lett. **112**, 155304 (2014).
[6] J. Ma, X. Wang, C. P. Sun, and Franco Nori, Quantum spin squeezing, Phys. Rep. **509**, 89 (2011).
[7] J. G. Bohnet, K. C. Cox, M. A. Norcia, J. M. Weiner, Z. Chen, and J. K. Thompson, Reduced spin measurement back-action for a phase sensitivity ten times beyond the standard quantum limit, Nat. Photonics **8**, 731 (2014).
[8] J. G. Bohnet, B. C. Sawyer, J. W. Britton, M. L. Wall, A. M. Rey, M. Foss-Feig, and J. J. Bollinger, Quantum spin dynamics and entanglement generation with hundreds of trapped ions, Science **352**, 1297 (2016).
[9] O. Hosten, R. Krishnakumar, N. J. Engelsen, and M. A. Kasevich, Quantum phase magnification, Science **352**, 1552 (2016).
[10] O. Hosten, N. J. Engelsen, R. Krishnakumar, and M. A. Kasevich, Measurement noise 100 times lower than the quantum-projection limit using entangled atoms, Nature (London) **529**, 505 (2016).
[11] X.-Y. Luo, Y.-Q. Zou, L.-N. Wu, Q. Liu, M.-F. Han, M. K. Tey, and L. You, Deterministic entanglement generation from driving through quantum phase transitions, Science **355**, 620 (2017).
[12] Y.-Q. Zou, L.-N. Wu, Q. Liu, X.-Y. Luo, S.-F. Guo, J.-H. Cao, M. K. Tey, and L. You, Beating the classical precision limit with spin-1 Dicke states of more than 10,000 atoms, Proc. Natl. Acad. Sci. U.S.A. **115**, 6381 (2018).
[13] H. Bao, J. Duan, S. Jin, X. Lu, P. Li, Weizhi Qu, M. Wang, I. Novikova, E. E. Mikhailov, K.-F. Zhao, K. Mlmer, H. Shen, and Y. Xiao, Spin squeezing of 10^{11} atoms by prediction and retrodiction measurements, Nature (London) **581**, 159 (2020).
[14] G.-B. Jo, Y. Shin, S. Will, T. A. Pasquini, M. Saba, W. Ketterle, D. E. Pritchard, M. Vengalattore, and M. Prentiss, Long Phase Coherence Time and Number Squeezing of Two Bose-Einstein Condensates on an Atom Chip, Phys. Rev. Lett. **98**, 030407 (2007).
[15] P. Berg, S. Abend, G. Tackmann, C. Schubert, E. Giese, W. P. Schleich, F. A. Narducci, W. Ertmer, and E. M. Rasel, Composite-Light-Pulse Technique for High-Precision Atom Interferometry, Phys. Rev. Lett. **114**, 063002 (2015).
[16] I. D. Leroux, M. H. Schleier-Smith, and V. Vuletić, Orientation-Dependent Entanglement Lifetime in a Squeezed Atomic Clock, Phys. Rev. Lett. **104**, 250801 (2010).
[17] E. M. Kessler, P. Kómár, M. Bishof, L. Jiang, A. S. Sørensen, J. Ye, and M. D. Lukin, Heisenberg-Limited Atom Clocks Based on Entangled Qubits, Phys. Rev. Lett. **112**, 190403 (2014).
[18] P. Kmr, E. M. Kessler, M. Bishof, L. Jiang, A. S. Srensen, J. Ye, and M. D. Lukin, A quantum network of clocks, Nat. Phys. **10**, 582 (2014).
[19] I. Kruse, K. Lange, J. Peise, B. Lücke, L. Pezzè, J. Arlt, W. Ertmer, C. Lisdat, L. Santos, A. Smerzi, and C. Klempt, Improvement of an Atomic Clock Using Squeezed Vacuum, Phys. Rev. Lett. **117**, 143004 (2016).
[20] E. Pedrozo-Peafiel, S. Colombo, C. Shu, A. F. Adiyatullin, Z. Li, E. Mendez, B. Braverman, A. Kawasaki, D. Akamatsu, Y. Xiao, and V. Vuleti, Entanglement on an optical atomic-clock transition, Nature (London) **588**, 414 (2020).
[21] R. J. Sewell, M. Koschorreck, M. Napolitano, B. Dubost, N. Behbood, and M. W. Mitchell, Magnetic Sensitivity beyond the Projection Noise Limit by Spin Squeezing, Phys. Rev. Lett. **109**, 253605 (2012).
[22] W. Muessel, H. Strobel, D. Linnemann, D. B. Hume, and M. K. Oberthaler, Scalable Spin Squeezing for Quantum-Enhanced Magnetometry with Bose-Einstein Condensates, Phys. Rev. Lett. **113**, 103004 (2014).
[23] S. S. Szigeti, S. P. Nolan, J. D. Close, and S. A. Haine, High-Precision Quantum-Enhanced Gravimetry with a

Bose-Einstein Condensate, Phys. Rev. Lett. **125**, 100402 (2020).
[24] Y. C. Liu, Z. F. Xu, G. R. Jin, and L. You, Spin Squeezing: Transforming One-Axis Twisting into Two-Axis Twisting, Phys. Rev. Lett. **107**, 013601 (2011).
[25] A. S. Sørensen and K. Mølmer, Entangling atoms in bad cavities, Phys. Rev. A **66**, 022314 (2002).
[26] X. Wang, A. Miranowicz, Y.-x. Liu, C. P. Sun, and F. Nori, Sudden vanishing of spin squeezing under decoherence, Phys. Rev. A **81**, 022106 (2010).
[27] P. Xue, Non-Markovian dynamics of spin squeezing, Phys. Lett. A **377**, 1328 (2013).
[28] Y.-C. Zhang, X.-F. Zhou, X. Zhou, G.-C. Guo, and Z.-W. Zhou, Cavity-Assisted Single-Mode and Two-Mode Spin-Squeezed States via Phase-Locked Atom-Photon Coupling, Phys. Rev. Lett. **118**, 083604 (2017).
[29] S. J. Masson and S. Parkins, Rapid Production of Many-Body Entanglement in Spin-1 Atoms via Cavity Output Photon Counting, Phys. Rev. Lett. **122**, 103601 (2019).
[30] W. Qin, Y.-H. Chen, X. Wang, A. Miranowicz, and F. Nori, Strong spin squeezing induced by weak squeezing of light inside a cavity, Nanophotonics **9**, 4853 (2020).
[31] P. Groszkowski, H.-K. Lau, C. Leroux, L. C. G. Govia, and A. A. Clerk, Heisenberg-Limited Spin Squeezing via Bosonic Parametric Driving, Phys. Rev. Lett. **125**, 203601 (2020).
[32] A. Kuzmich, L. Mandel, and N. P. Bigelow, Generation of Spin Squeezing via Continuous Quantum Nondemolition Measurement, Phys. Rev. Lett. **85**, 1594 (2000).
[33] J. Appel, P. J. Windpassinger, D. Oblak, U. B. Hoff, N. Kjærgaard, and E. S. Polzik, Mesoscopic atomic entanglement for precision measurements beyond the standard quantum limit, Proc. Natl. Acad. Sci. U.S.A. **106**, 10960 (2009).
[34] M. Kritsotakis, J. A. Dunningham, and S. A. Haine, Spin squeezing of a Bose-Einstein condensate via a quantum nondemolition measurement for quantum-enhanced atom interferometry, Phys. Rev. A **103**, 023318 (2021).
[35] T. Lund-Hansen, S. Stobbe, B. Julsgaard, H. Thyrrestrup, T. Sünner, M. Kamp, A. Forchel, and P. Lodahl, Experimental Realization of Highly Efficient Broadband Coupling of Single Quantum Dots to a Photonic Crystal Waveguide, Phys. Rev. Lett. **101**, 113903 (2008).
[36] A. F. van Loo, A. Fedorov, K. Lalumière, B. C. Sanders, A. Blais, and A. Wallraff, Photon-mediated interactions between distant artificial atoms, Science **342**, 1494 (2013).
[37] J. Petersen, J. Volz, and A. Rauschenbeutel, Chiral nanophotonic waveguide interface based on spin-orbit interaction of light, Science **346**, 67 (2014).
[38] R. Mitsch, C. Sayrin, B. Albrecht, P. Schneeweiss, and A. Rauschenbeutel, Quantum state-controlled directional spontaneous emission of photons into a nanophotonic waveguide, Nat. Commun. **5**, 5713 (2014).
[39] A. Sipahigil, R. E. Evans, D. D. Sukachev, M. J. Burek, J. Borregaard, M. K. Bhaskar, C. T. Nguyen, J. L. Pacheco, H. A. Atikian, C. Meuwly, R. M. Camacho, F. Jelezko, E. Bielejec, H. Park, M. Lončar, and M. D. Lukin, An integrated diamond nanophotonics platform for quantum-optical networks, Science **354**, 847 (2016).
[40] B. Kannan, M. J. Ruckriegel, D. L. Campbell, A. F. Kockum, J. Braumller, D. K. Kim, M. Kjaergaard, P. Krantz, A. Melville, B. M. Niedzielski, A. Vepslinen, R. Winik, J. L. Yoder, F. Nori, T. P. Orlando, S. Gustavsson, and W. D. Oliver, Waveguide quantum electrodynamics with superconducting artificial giant atoms, Nature (London) **583**, 775 (2020).
[41] B. Kannan, D. L. Campbell, F. Vasconcelos, R. Winik, D. K. Kim, M. Kjaergaard, P. Krantz, A. Melville, B. M. Niedzielski, J. L. Yoder, T. P. Orlando, S. Gustavsson, and W. D. Oliver, Generating spatially entangled itinerant photons with waveguide quantum electrodynamics, Sci. Adv. **6**, eabb8780 (2020).
[42] E. Kim, X. Zhang, V. S. Ferreira, J. Banker, J. K. Iverson, A. Sipahigil, M. Bello, A. González-Tudela, M. Mirhosseini, and O. Painter, Quantum Electrodynamics in a Topological Waveguide, Phys. Rev. X **11**, 011015 (2021).
[43] M.-A. Lemonde, S. Meesala, A. Sipahigil, M. J. A. Schuetz, M. D. Lukin, M. Loncar, and P. Rabl, Phonon Networks with Silicon-Vacancy Centers in Diamond Waveguides, Phys. Rev. Lett. **120**, 213603 (2018).
[44] H. Krauter, C. A. Muschik, K. Jensen, W. Wasilewski, J. M. Petersen, J. Ignacio Cirac, and E. S. Polzik, Entanglement Generated by Dissipation and Steady State Entanglement of Two Macroscopic Objects, Phys. Rev. Lett. **107**, 080503 (2011).
[45] E. Shahmoon and G. Kurizki, Nonradiative interaction and entanglement between distant atoms, Phys. Rev. A **87**, 033831 (2013).
[46] A. Gonzalez-Tudela, D. Martin-Cano, E. Moreno, L. Martin-Moreno, C. Tejedor, and F. J. Garcia-Vidal, Entanglement of Two Qubits Mediated by One-Dimensional Plasmonic Waveguides, Phys. Rev. Lett. **106**, 020501 (2011).
[47] A. González-Tudela and D. Porras, Mesoscopic Entanglement Induced by Spontaneous Emission in Solid-State Quantum Optics, Phys. Rev. Lett. **110**, 080502 (2013).
[48] A. González-Tudela, V. Paulisch, D. E. Chang, H. J. Kimble, and J. I. Cirac, Deterministic Generation of Arbitrary Photonic States Assisted by Dissipation, Phys. Rev. Lett. **115**, 163603 (2015).
[49] E. G. Dalla Torre, J. Otterbach, E. Demler, V. Vuletic, and M. D. Lukin, Dissipative Preparation of Spin Squeezed Atomic Ensembles in a Steady State, Phys. Rev. Lett. **110**, 120402 (2013).
[50] W. Song, W. Yang, J. An, and M. Feng, Dissipation-assisted spin squeezing of nitrogen-vacancy centers coupled to a rectangular hollow metallic waveguide, Opt. Express **25**, 19226 (2017).
[51] Y.-F. Qiao, H.-Z. Li, X.-L. Dong, J.-Q. Chen, Y. Zhou, and P.-B. Li, Phononic-waveguide-assisted steady-state entanglement of silicon-vacancy centers, Phys. Rev. A **101**, 042313 (2020).
[52] D. Kienzler, H.-Y. Lo, B. Keitch, L. de Clercq, F. Leupold, F. Lindenfelser, M. Marinelli, V. Negnevitsky, and J. P. Home, Quantum harmonic oscillator state synthesis by reservoir engineering, Science **347**, 53 (2015).
[53] A. Metelmann and A. A. Clerk, Nonreciprocal Photon Transmission and Amplification via Reservoir Engineering, Phys. Rev. X **5**, 021025 (2015).
[54] H. R. Haakh and S. Scheel, Modified and controllable dispersion interaction in a one-dimensional waveguide geometry, Phys. Rev. A **91**, 052707 (2015).
[55] K. V. Kepesidis, M.-A. Lemonde, A. Norambuena, J. R. Maze, and P. Rabl, Cooling phonons with phonons:

Acoustic reservoir engineering with silicon-vacancy centers in diamond, Phys. Rev. B **94**, 214115 (2016).
[56] Y. Yanay and A. A. Clerk, Reservoir engineering of bosonic lattices using chiral symmetry and localized dissipation, Phys. Rev. A **98**, 043615 (2018).
[57] J. Roßnagel, O. Abah, F. Schmidt-Kaler, K. Singer, and E. Lutz, Nanoscale Heat Engine beyond the Carnot Limit, Phys. Rev. Lett. **112**, 030602 (2014).
[58] C.-J. Yang, J.-H. An, W. Yang, and Y. Li, Generation of stable entanglement between two cavity mirrors by squeezed-reservoir engineering, Phys. Rev. A **92**, 062311 (2015).
[59] S. Zeytinoğlu, A. İmamoğlu, and S. Huber, Engineering Matter Interactions Using Squeezed Vacuum, Phys. Rev. X **7**, 021041 (2017).
[60] S. Kono, Y. Masuyama, T. Ishikawa, Y. Tabuchi, R. Yamazaki, K. Usami, K. Koshino, and Y. Nakamura, Nonclassical Photon Number Distribution in a Superconducting Cavity under a Squeezed Drive, Phys. Rev. Lett. **119**, 023602 (2017).
[61] W. Qin, A. Miranowicz, P.-B. Li, X.-Y. Lü, J. Q. You, and F. Nori, Exponentially Enhanced Light-Matter Interaction, Cooperativities, and Steady-State Entanglement Using Parametric Amplification, Phys. Rev. Lett. **120**, 093601 (2018).
[62] S. Zippilli and D. Vitali, Dissipative Engineering of Gaussian Entangled States in Harmonic Lattices with a Single-Site Squeezed Reservoir, Phys. Rev. Lett. **126**, 020402 (2021).
[63] T. E. Lee, S. Gopalakrishnan, and M. D. Lukin, Unconventional Magnetism via Optical Pumping of Interacting Spin Systems, Phys. Rev. Lett. **110**, 257204 (2013).
[64] Y. Liu and A. A. Houck, Quantum electrodynamics near a photonic bandgap, Nat. Phys. **13**, 48 (2017).
[65] L. Krinner, M. Stewart, A. Pazmiño, J. Kwon, and D. Schneble, Spontaneous emission of matter waves from a tunable open quantum system, Nature (London) **559**, 589 (2018).
[66] C. Chen, C.-J. Yang, and J.-H. An, Exact decoherence-free state of two distant quantum systems in a non-Markovian environment, Phys. Rev. A **93**, 062122 (2016).
[67] Y. Fang and M. Sun, Nanoplasmonic waveguides: Towards applications in integrated nanophotonic circuits, Light **4**, e294 (2015).
[68] C.-J. Yang, J.-H. An, and H.-Q. Lin, Signatures of quantized coupling between quantum emitters and localized surface plasmons, Phys. Rev. Research **1**, 023027 (2019).
[69] H. S. Dutta, A. K. Goyal, V. Srivastava, and S. Pal, Coupling light in photonic crystal waveguides: A review, Photonics Nanostruct. Fundamen. Appl. **20**, 41 (2016).
[70] H. Vahlbruch, M. Mehmet, K. Danzmann, and R. Schnabel, Detection of 15 db Squeezed States of Light and their Application for the Absolute Calibration of Photoelectric Quantum Efficiency, Phys. Rev. Lett. **117**, 110801 (2016).
[71] T. Serikawa, J. i. Yoshikawa, K. Makino, and A. Frusawa, Creation and measurement of broadband squeezed vacuum from a ring optical parametric oscillator, Opt. Express **24**, 28383 (2016).
[72] J. Bourassa, F. Beaudoin, J. M. Gambetta, and A. Blais, Josephson-junction-embedded transmission-line resonators: From kerr medium to in-line transmon, Phys. Rev. A **86**, 013814 (2012).
[73] C. Macklin, K. O'Brien, D. Hover, M. E. Schwartz, V. Bolkhovsky, X. Zhang, W. D. Oliver, and I. Siddiqi, A near–quantum-limited josephson traveling-wave parametric amplifier, Science **350**, 307 (2015).
[74] H.-P. Breuer and F. Petruccione, *The Theory of Open Quantum Systems* (Oxford University Press, Oxford, 2007).
[75] H. Mäkelä and M. Möttönen, Effects of the rotating-wave and secular approximations on non-Markovianity, Phys. Rev. A **88**, 052111 (2013).
[76] See Supplemental Material at http://link.aps.org/supplemental/10.1103/PhysRevLett.127.083602 for a detailed derivation of the master equation, its reduction to the form of the collective spin, the steady-state solution, the derivation of scaling relation of r_{opt}, and the analysis of the weak position disorder.
[77] E. Pucci, A. U. Zaman, E. Rajo-Iglesias, P.-S. Kildal, and A. Kishk, Study of q-factors of ridge and groove gap waveguide resonators, IET Microwav. Antennas Propagat. **7**, 900 (2013).
[78] J. Au Kong, *Electromagnetic Wave Theory* (John Wiley and Sons, New York, 1986).
[79] G. Tóth, C. Knapp, O. Gühne, and H. J. Briegel, Spin squeezing and entanglement, Phys. Rev. A **79**, 042334 (2009).
[80] U. Leonhardt and H. Paul, Phase measurement and Q function, Phys. Rev. A **47**, R2460 (1993).
[81] G. S. Agarwal and R. R. Puri, Cooperative behavior of atoms irradiated by broadband squeezed light, Phys. Rev. A **41**, 3782 (1990).
[82] C. Gross, Spin squeezing, entanglement and quantum metrology with Bose–Einstein condensates, J. Phys. B **45**, 103001 (2012).
[83] G. Tóth and I. Apellaniz, Quantum metrology from a quantum information science perspective, J. Phys. A **47**, 424006 (2014).
[84] V. Giovannetti, S. Lloyd, and L. Maccone, Advances in quantum metrology, Nat. Photonics **5**, 222 (2011).
[85] T. E. Lee, F. Reiter, and N. Moiseyev, Entanglement and Spin Squeezing in Non-Hermitian Phase Transitions, Phys. Rev. Lett. **113**, 250401 (2014).
[86] S. Dusuel and J. Vidal, Finite-Size Scaling Exponents of the Lipkin-Meshkov-Glick Model, Phys. Rev. Lett. **93**, 237204 (2004).
[87] A. Mohan, P. Gallo, M. Felici, B. Dwir, A. Rudra, J. Faist, and E. Kapon, Record-low inhomogeneous broadening of site-controlled quantum dots for nanophotonics, Small **6**, 1268 (2010).
[88] M. Felici, G. Pettinari, F. Biccari, A. Boschetti, S. Younis, S. Birindelli, M. Gurioli, A. Vinattieri, A. Gerardino, L. Businaro, M. Hopkinson, S. Rubini, M. Capizzi, and A. Polimeni, Broadband enhancement of light-matter interaction in photonic crystal cavities integrating site-controlled quantum dots, Phys. Rev. B **101**, 205403 (2020).
[89] J. Wang, Y. Zhou, X. Zhang, F. Liu, Y. Li, K. Li, Z. Liu, G. Wang, and W. Gao, Efficient Generation of an Array of Single Silicon-Vacancy Defects in Silicon Carbide, Phys. Rev. Applied **7**, 064021 (2017).

Correction: The caption to Figure 1 contained a typographical error and has been fixed.